

The Effective Action for Local Composite Operators $\Phi^2(x)$ and $\Phi^4(x)$

Anna Okopińska

Institute of Physics, Warsaw University, Białystok Branch,
Lipowa 41, 15-424 Białystok, Poland
e-mail: rozynek@fuw.edu.pl

Abstract

The generating functionals for the local composite operators, $\Phi^2(x)$ and $\Phi^4(x)$, are used to study excitations in the scalar quantum field theory with $\lambda\Phi^4$ interaction. The effective action for the composite operators is obtained as a series in the Planck constant \hbar , and the two- and four-particle propagators are derived. The numerical results are studied in the space-time of one dimension, when the theory is equivalent to the quantum mechanics of an anharmonic oscillator. The effective potential and the poles of the composite propagators are obtained as series in \hbar , with effective mass and coupling determined by non-perturbative gap equations. This provides a systematic approximation method for the ground state energy, and for the second and fourth excitations. The results show quick convergence to the exact values, better than that obtained without including the operator Φ^4 .

1 Introduction

The quantum mechanical anharmonic oscillator (AO) can be regarded as a quantum field theory of a real scalar field with a classical action given by

$$S[\Phi] = \int [\frac{1}{2}\Phi(x)(-\partial^2 + m^2)\Phi(x) + \lambda\Phi^4(x)] d^n x, \quad (1)$$

when the dimension of the Euclidean space-time n is equal to one. For this reason the AO is frequently used as a testing ground for approximation methods in quantum field theory. The field-theoretical perturbation method enables us to calculate Green's functions and their generating functionals to an arbitrary order in the coupling constant λ . Within this approach the perturbative expansion of the ground state energy of the AO is easily obtained by calculating the effective potential in the loop expansion, but a derivation of excitation energies from zero modes of the appropriate Green's functions is not so straightforward [1], in contrast to the Schrödinger approach, where perturbative calculations for excited levels are of the same difficulty as for the ground state.

For a field-theoretical investigation of excited modes, the N -particle functionals which depend on some artificial sources coupled to composite operators, $\Phi(x_1)\Phi(x_2)\dots\Phi(x_N)$, have been introduced [2, 3]. These functionals generate composite propagators through differentiation with respect to the sources. The simplest Green's functions, with the simplest relations to multi-particle eigenmodes, are generated by the effective action for composite operators, defined through a Legendre transform of the connected generating functional. For $N \leq 4$ the effective action has been shown [3, 4] to be a sum of N -particle-irreducible vacuum diagrams with the exact propagator. In the case $N = 2$, studied in the classic paper of Cornwall, Jackiw and Tomboulis [5], the Gaussian effective action (and the Gaussian effective potential [6]) is obtained as an approximation of the two-loop result. It is, however, difficult to discuss a full content of the two-loop result, and to proceed to higher operators within such an approach because of the highly non-trivial integral gap equations for vacuum expectation values of composite fields.

The local N -particle operators $\Phi^N(x)$ have been also considered [7]; however, diagrammatic rules for the effective action were lacking, since the Legendre transform cannot be performed explicitly in this case. Only recently,

an expansion of the effective action for the operator $\Phi^2(x)$ in terms of two-particle-point-irreducible (2PPI) diagrams was given [8, 9]. The result is implicit but enables us to calculate the effective potential [9] and the two-particle composite propagator [10]. The Gaussian effective action is obtained already in the one-loop approximation, and the calculation of post-Gaussian corrections is easier than for the bilocal operator, since the gap equation for the vacuum expectation value of the local composite field is algebraic. Unfortunately this approach cannot be extended to $N > 2$, and all one can do in that case is to perform the inversion in the Legendre transform order by order in the Planck constant \hbar . For multilocal operators this uphill task can be done explicitly, and the well-known expansions in N -particle-irreducible diagrams are recovered [11]. For the local composite operator $\Phi^2(x)$ the method appears implicit; nevertheless it makes a discussion of many applications possible [12, 13]. Even the diagrammatic rules for the effective action (different from that of the 2PPI expansion) have been established [11, 14]. The aim of our paper is to extend the inversion method to include the composite operator $\Phi^4(x)$.

In Section 2, after a brief exposition of the generating functionals for composite operators, a diagrammatic representation of the effective action for the $\Phi^2(x)$ operator is obtained explicitly to the order \hbar^5 , and the (inverse) two-particle composite propagator is derived up to \hbar^4 . Then we calculate the effective action for two operators, $\Phi^2(x)$ and $\Phi^4(x)$, to the order \hbar^4 . This enables us to obtain the two- and four-particle propagators up to \hbar^3 and \hbar^2 , respectively. Having in mind an application of the formalism in relativistic quantum field theory, we discuss the scalar theory in the space-time of n -dimensions, keeping n arbitrary as long as possible. It is only in Section 3, when calculating excitation energies, that we set $n = 1$ to consider the AO. The poles of the composite propagators are determined in successive orders of \hbar and the resulting energies are compared with the exact spectrum of the oscillator. The approximations for the ground state energy and for the second excitation, obtained from the effective action for $\Phi^2(x)$, are in good agreement with the exact results; however, in this approach there is no simple way to derive the fourth excitation. The advantage of using the effective action for two operators, $\Phi^2(x)$ and $\Phi^4(x)$, lies in the fact that it generates directly the four-particle propagator, providing an excellent approximation to the fourth excitation energy of the AO. Moreover, the approximations to the ground state and to the second excitation obtained from the effective action

for the operators $\Phi^2(x)$ and $\Phi^4(x)$ are considerably better than that obtained from the effective action for the operator $\Phi^2(x)$ only. Our conclusions are summarized in Section 4.

2 The effective action for local composite operators through the inversion method

2.1 Generating functionals for composite operators

The vacuum functional for the local composite operators $\Phi^2(x)$ and $\Phi^4(x)$ can be represented by a path integral

$$Z[J, K] = e^{\frac{1}{\hbar}W[J, K]} = \int D\Phi e^{\frac{1}{\hbar}[-S[\Phi] + \frac{1}{2} \int J(x)\Phi^2(x) d^n x + \frac{1}{24} \int K(x)\Phi^4(x) d^n x]}. \quad (2)$$

The connected generating functional, $W[J, K]$, is given by a sum of vacuum diagrams in configuration space, obtained with an inverse propagator $G_J^{-1}(x, y) = (-\partial^2 + m^2 - J(x))\delta(x - y)$ and a four-point vertex given by $(K(x) - 24\lambda)\delta(x - y)\delta(x - w)\delta(x - z)$; in Fig. ?? we show the diagrammatic expansion to the order \hbar^5 . For simplicity, we consider here the case of unbroken reflection symmetry, when the vacuum expectation value of the scalar field vanishes; this is why we do not introduce a current coupled to an elementary field $\Phi(x)$. This, however, will limit our investigation to the even excitations of the system.

The effective action is defined through a Legendre transform

$$\begin{aligned} \Gamma[\Delta, \Lambda] &= W[J, K] - \frac{\hbar}{2} \int J(x)\Delta(x) d^n x - \frac{\hbar^3}{24} \int K(x)\Lambda(x) d^n x \\ &\quad - \frac{\hbar^2}{8} \int K(x)\Delta^2(x) d^n x, \end{aligned} \quad (3)$$

where the background fields are defined as

$$\begin{aligned} \hbar\Delta(x) &= 2 \frac{\delta W}{\delta J(x)} = \langle \Phi^2(x) \rangle_{J, K} \\ \hbar^3\Lambda(x) &= 24 \frac{\delta W}{\delta K(x)} - 3\hbar^2\Delta^2(x) = \langle \Phi^4(x) \rangle_{J, K} - 3 \langle \Phi^2(x) \rangle_{J, K}^2 \end{aligned} \quad (4)$$

and $\langle \dots \rangle_{J,K}$ denotes the expectation value in the presence of external currents $J(x)$ and $K(x)$.

The external sources J and K were introduced artificially in order to define the background fields (4) and the effective action as a functional of those (3). The physical quantities have to be calculated at $J = K = 0$, or equivalently at the values of the background fields, Δ and Λ , for which the gap equations

$$\frac{\delta\Gamma}{\delta\Delta(x)} = -\frac{\hbar}{2}J(x) - \frac{\hbar^2}{4}\Delta(x)K(x) = 0, \quad (5)$$

$$\frac{\delta\Gamma}{\delta\Lambda(x)} = -\frac{\hbar^3}{24}K(x) = 0 \quad (6)$$

are satisfied. The effective action for the composite operators, $\Gamma[\Delta, \Lambda]$, determines the vacuum energy density

$$E_0 = - \left. \frac{\Gamma[\Delta, \Lambda]}{\int d^n x} \right|_{\Delta=\text{const}, \Lambda=\text{const}}. \quad (7)$$

If another solution to the gap equations ($\Delta(x) = \Delta + D\Delta(x)$, $\Lambda(x) = \Lambda + D\Lambda(x)$) exists in the vicinity of (Δ, Λ) , then by (5) and (6) the stability condition [7, 15] is obtained in the form

$$f \left| \begin{array}{cc} \Gamma_{22}(x, y) & \Gamma_{24}(x, y) \\ \Gamma_{42}(x, y) & \Gamma_{44}(x, y) \end{array} \right| \left| \begin{array}{c} D\Delta(y) \\ D\Lambda(y) \end{array} \right| dy = \left| \begin{array}{c} 0 \\ 0 \end{array} \right|. \quad (8)$$

The matrix Γ , given by

$$\begin{aligned} \Gamma_{22}(x, y) &= \left. \frac{\delta^2\Gamma}{\delta\Delta(x)\delta\Delta(y)} \right|_{\Delta, \Lambda} = -\frac{\hbar}{2} \frac{\delta \left(J(x) + \frac{\hbar}{2}K(x)\Delta(x) \right)}{\delta\Delta(y)} \Big|_{\Delta, \Lambda} \\ \Gamma_{24}(x, y) &= \Gamma_{42}(x, y) = \left. \frac{\delta^2\Gamma}{\delta\Delta(x)\delta\Lambda(y)} \right|_{\Delta, \Lambda} = -\frac{\hbar^3}{24} \frac{\delta K(x)}{\delta\Delta(y)} \Big|_{\Delta, \Lambda} \\ \Gamma_{44}(x, y) &= \left. \frac{\delta^2\Gamma}{\delta\Lambda(x)\delta\Lambda(y)} \right|_{\Delta, \Lambda} = -\frac{\hbar^3}{24} \frac{\delta K(x)}{\delta\Lambda(y)} \Big|_{\Delta, \Lambda}, \end{aligned} \quad (9)$$

is an inverse of the composite propagator matrix, defined as

$$W(x, y) = \left| \begin{array}{cc} W_{22}(x, y) & W_{24}(x, y) \\ W_{42}(x, y) & W_{44}(x, y) \end{array} \right| = \left| \begin{array}{cc} \frac{\delta^2 W}{\delta J(x)\delta J(y)} \Big|_{0,0} & \frac{\delta^2 W}{\delta J(x)\delta K(y)} \Big|_{0,0} \\ \frac{\delta^2 W}{\delta K(x)\delta J(y)} \Big|_{0,0} & \frac{\delta^2 W}{\delta K(x)\delta K(y)} \Big|_{0,0} \end{array} \right|$$

$$= \begin{vmatrix} \langle T\Phi^2(x)\Phi^2(y) \rangle_{con} & \langle T\Phi^2(x)\Phi^4(y) \rangle_{con} \\ \langle T\Phi^4(x)\Phi^2(y) \rangle_{con} & \langle T\Phi^4(x)\Phi^4(y) \rangle_{con} \end{vmatrix}. \quad (10)$$

In Fourier space the stability condition (8) is written as

$$\begin{vmatrix} \Gamma_{22}(p) & \Gamma_{24}(p) \\ \Gamma_{42}(p) & \Gamma_{44}(p) \end{vmatrix} \begin{vmatrix} D\Delta(p) \\ D\Lambda(p) \end{vmatrix} = \begin{vmatrix} 0 \\ 0 \end{vmatrix}, \quad (11)$$

hence the zero modes of $\Gamma(p)$ are related to the excitations of the system. The matrix $\Gamma(p)$ can be diagonalised, providing the inverse of the two-particle propagator in the form

$$\hbar\Gamma^4(p) = \Gamma_{22}(p) - \Gamma_{24}(p)\Gamma_{44}^{-1}(p)\Gamma_{42}(p) \quad (12)$$

and that of the four-particle propagator equal to

$$\hbar^3\Gamma^8(p) = \Gamma_{44}(p) - \Gamma_{42}(p)\Gamma_{22}^{-1}(p)\Gamma_{24}(p). \quad (13)$$

The effective action for the composite operators, $\Gamma[\Delta, \Lambda]$, provides a convenient tool to study the ground state and excitations. Unfortunately, a systematic approximation scheme for the effective action is intricate, although the connected generating functional, $W[J, K]$, can be easily obtained in terms of Feynman diagrams in the loop expansion. The main difficulty lies in performing the Legendre transform (3), i.e. in eliminating the sources J and K in favour of Δ and Λ . Here we shall do this order by order in \hbar , representing the vacuum expectation values Δ and Λ by the series

$$\Delta = \sum_{k=0}^{\infty} \hbar^k \Delta_{(k)}[J, K], \quad (14)$$

$$\Lambda = \sum_{k=0}^{\infty} \hbar^k \Lambda_{(k)}[J, K], \quad (15)$$

where the coefficients $\Delta_k[J, K]$ and $\Lambda_k[J, K]$ can be easily found from Eq. 4. The diagrammatic representation of Δ and Λ to the order \hbar^4 and \hbar^2 respectively is given in Fig. ???. The inverted series are written as

$$J = \sum_{k=0}^{\infty} \hbar^k J_{(k)}[\Delta, \Lambda], \quad (16)$$

$$K = \sum_{k=0}^{\infty} \hbar^k K_{(k)}[\Delta, \Lambda], \quad (17)$$

and the coefficients $J_{(k)}[\Delta, \Lambda]$ and $K_{(k)}[\Delta, \Lambda]$ have to be determined order by order in \hbar . It has to be noted that only the lowest-order inverse functionals, $J_0[\Delta, \Lambda]$ and $K_0[\Delta, \Lambda]$, are required; higher order coefficients are obtained as functionals of them. This establishes an algorithm for calculating the effective action to an arbitrary order in \hbar even if $J_0[\Delta, \Lambda]$ and $K_0[\Delta, \Lambda]$ cannot be obtained explicitly, which is the case for local composite operators.

2.2 The effective action for $\Phi^2(x)$, $\Gamma[\Delta]$

The effective action for the two-particle operator $\Phi^2(x)$, $\Gamma[\Delta]$, has been recently examined with great care by Okumura [11] and Yokojima [14]. As an introduction to the case of four-particle operator, discussed in the next section, we review here the calculation of $\Gamma[\Delta]$ by performing the Legendre transform of the connected generating functional $W[J]$ to the order \hbar^5 . In the definition of the effective action for the two-particle operator, $\Gamma[\Delta]$, only the current $J(x)$ coupled to $\Phi^2(x)$ is required; therefore $K(x)$ has to be set to zero in the formulas for the generating functionals (2-??) and only Eq. (14) has to be inverted, to determine a functional $J[\Delta]$ to the given order in \hbar . Using the identity

$$\Delta = \sum_{k=0}^{\infty} \hbar^k \Delta_{(k)} \left[\sum_{i=0}^{\infty} \hbar^i J_{(i)}[\Delta] \right], \quad (18)$$

one obtains an infinite sequence of equations

$$\Delta = \Delta_{(0)} \quad (19)$$

$$\Delta'_{(0)} J_{(1)} + \Delta_{(1)} = 0, \quad (20)$$

$$\Delta'_{(0)} J_{(2)} + \frac{1}{2} \Delta''_{(0)} (J_{(1)})^2 + \Delta'_{(1)} J_{(1)} + \Delta_{(2)} = 0, \quad (21)$$

$$\begin{aligned} & \Delta'_{(0)} J_{(3)} + \Delta''_{(0)} J_{(1)} J_{(2)} \\ & + \frac{1}{3!} \Delta'''_{(0)} (J_{(1)})^3 + \Delta'_{(1)} J^{(2)} + \frac{1}{2} \Delta''_{(1)} (J_{(1)})^2 + \Delta_{(3)} = 0, \end{aligned} \quad (22)$$

$$\begin{aligned}
& \Delta'_{(0)} J^{(4)} + \frac{1}{2} \Delta''_{(0)} (2J_{(1)} J^{(3)} + (J_{(2)})^2) \\
& + \frac{1}{2} \Delta'''_{(0)} (J_{(1)})^2 J_{(2)} + \frac{1}{4!} \Delta''''_{(0)} (J_{(1)})^4 + \Delta'_{(1)} J^{(3)} + \frac{1}{3!} \Delta'''_{(1)} (J_{(1)})^3 \\
& + \Delta''_{(1)} J_{(1)} J_{(2)} + \Delta'_{(2)} J_{(2)} + \frac{1}{2} \Delta''_{(2)} (J_{(1)})^2 + \Delta'_{(3)} J_{(1)} + \Delta_{(4)} = 0 \quad (23)
\end{aligned}$$

...

where $\Delta_{(k)}[J_0]$ are given in Fig. ???. Here and in the following the space-time indices and integration over them are suppressed for notational simplicity. The coefficients $J_{(i)}$, calculated from Eqs. 20- 23, can be represented by Feynman diagrams in configuration space with the (inverse) free propagator

$$G_{J_0}^{-1}(x, y) = (-\partial + \Omega^2(x))\delta(x - y), \quad (24)$$

where

$$\Omega^2[\Delta] = m^2 - J_0[\Delta]. \quad (25)$$

The result to the order \hbar^4 is shown in Fig. ??; the inverse two-particle propagator, attached to an external point, is that of two free particles of an effective mass $\Omega(x)$. In Fig. ?? we show the effective action $\Gamma[\Delta]$ to the order \hbar^5 , obtained by eliminating J with the use of Fig. ??. In agreement with the rule proved by Okumura [11], $\Gamma[\Delta]$ appears to be a sum of one-vertex-irreducible diagrams with the inverse composite propagator attached to an external point, and the two-point pseudo-vertices $J_{(i)}$ of order i ($i \geq 2$) inserted in all possible ways. By way of digression, it can be observed that all pseudo-vertex insertions in $\Gamma[\Delta]$ can be summed by taking a dressed inverse propagator in the form $G_{sum}^{-1}(x, y) = (-\partial^2 + m^2 - J_0(x) - J_2(x) - J_3(x) - J_4(x) + \dots)\delta(x - y) = (-\partial^2 + m^2 - J(x) + J_1(x))\delta(x - y)$, and the result coincides with that obtained in the 2PPI expansion [9] which establishes a relation between the two methods.

The definition of the effective action $\Gamma[\Delta]$ is implicit, since the functional

$$\Delta[J_0](x) = G_{J_0}(x, x), \quad (26)$$

obtained from (19), cannot be inverted for a space-time dependent J_0 . However, using the fact that all dependence on J is through J_0 , Eq.26 enables us to calculate $\left. \frac{\delta J_0(z)}{\delta \Delta(y)} \right|_{\Delta(x)=\Delta}$, and hence the two-particle inverse propagator

$$\Gamma^4(x - y) = \Gamma_{22}(x - y) = - \frac{\hbar}{2} \int d^n z \frac{\delta J(x)}{\delta J_0(z)} \frac{\delta J_0(z)}{\delta \Delta(y)} \Big|_{\Delta(x)=\Delta}. \quad (27)$$

Since a constant Δ corresponds to constant Ω , the vacuum energy density (7), as well as the Fourier transform of the two-particle two-point Green's function, $\Gamma^4(p)$, can be represented by the Feynman diagrams in momentum space with the propagator $\frac{1}{p^2 + \Omega^2}$. The vacuum energy density is given by the same set of diagrams as the effective action (Fig. ??), but in momentum space. The result for $\Gamma^4(p)$ calculated from (27) to the order \hbar^3 is shown in Fig. ?. In this case (19) can be written as

$$\Delta = \int \frac{d^n p}{(2\pi)^n} \frac{1}{p^2 + \Omega^2}, \quad (28)$$

and can be used to eliminate Δ in favor of Ω in all the quantities considered. The gap equation (5), which becomes algebraic, determines the value of Ω which corresponds to vanishing external current.

2.3 The effective action for $\Phi^2(x)$ and $\Phi^4(x)$ operators, $\Gamma[\Delta, \Lambda]$

In order to calculate the effective action for the operators $\Phi^2(x)$ and $\Phi^4(x)$, $\Gamma[\Delta, \Lambda]$, both the series given by (14) and (15) have to be inverted. Using the identities

$$\Delta = \sum_{k=0}^{\infty} \hbar^k \Delta_{(k)} \left[\sum_{i=0}^{\infty} \hbar^i J_{(i)}[\Delta, \Lambda], \sum_{k=0}^{\infty} \hbar^i K_{(i)}[\Delta, \Lambda] \right]. \quad (29)$$

and

$$\Lambda = \sum_{k=0}^{\infty} \hbar^k \Lambda_{(k)} \left[\sum_{i=0}^{\infty} \hbar^i J_{(i)}[\Delta, \Lambda], \sum_{i=0}^{\infty} \hbar^i K_{(i)}[\Delta, \Lambda] \right]. \quad (30)$$

we obtain two infinite sequences of equations

$$\Delta = \Delta_{(0)} \quad (31)$$

$$\frac{\delta \Delta_{(0)}}{\delta J_0} J_1 + \Delta_{(1)} = 0, \quad (32)$$

$$\frac{\delta \Delta_{(0)}}{\delta J_0} J_{(2)} + \frac{1}{2} \frac{\delta^2 \Delta_{(0)}}{\delta J_0^2} (J_{(1)})^2 + \frac{\delta \Delta_{(1)}}{\delta J_0} J_{(1)} + \frac{\delta \Delta_{(1)}}{\delta K_0} K_{(1)} + \Delta_{(2)} = 0, \quad (33)$$

...

and

$$\Lambda = \Lambda_{(0)} \quad (34)$$

$$\frac{\delta\Lambda_{(0)}}{\delta J_0} J_1 + \frac{\delta\Lambda_{(0)}}{\delta K_0} K_1 + \Lambda_{(1)} = 0, \quad (35)$$

$$\frac{\delta\Lambda_{(0)}}{\delta J_0} J_{(2)} + \frac{1}{2} \frac{\delta^2\Lambda_{(0)}}{\delta J_0^2} (J_{(1)})^2 + \frac{\delta\Lambda_{(0)}}{\delta K_0} K_{(2)} + \frac{\delta^2\Lambda_{(0)}}{\delta J_0 \delta K_0} J_{(1)} K_{(1)} + \frac{\delta\Lambda_{(1)}}{\delta J_0} J_{(1)} + \Lambda_{(2)} = 0, \quad (36)$$

...,

where we made use of the fact that $\Delta_{(0)}$ and $\frac{\delta\Lambda_{(0)}}{\delta K_0}$ do not depend on K_0 . Taking $\Delta_{(k)}[J_0, K_0]$ and $\Lambda_{(k)}[J_0, K_0]$ from Fig. ??, we calculated the coefficients $J_{(i)}$ and $K_{(i)}$, from the above equations. The results for J and K to the order \hbar^3 and \hbar^2 respectively are represented in Fig. ?? by Feynman diagrams in configuration space, where the composite propagators are those of two or four free particles. The effective mass in a free propagator, $\Omega[\Delta]$ (25), is the same as in the case of $\Gamma[\Delta]$ considered in Section 2.2, and the four-point vertex is $(K_0(x) - 24\lambda)\delta(x-y)\delta(x-w)\delta(x-z)$. In Fig. ?? we show the effective action, $\Gamma[\Delta, \Lambda]$ to the order \hbar^4 , which is obtained as a Legendre transform of the connected generating functional by using Fig. ?? to eliminate J and K in favour of Δ and Λ . It seems that, as in the case of $\Gamma[\Delta]$, graphical rules could be established, but we do not discuss this point here.

The expression for $\Gamma[\Delta, \Lambda]$ given in Fig. ?? is implicit, with the relations for $J_0[\Delta, \Lambda]$ and $K_0[\Delta, \Lambda]$ given by (31) and (34) respectively. The vacuum energy density (7) is represented by the same set of Feynman diagrams as the effective action (Fig. ??), but in momentum space with the propagator $\frac{1}{p^2 + \Omega^2}$. Using the fact that all dependence on sources is through J_0 and K_0 , the implicit expression for $\Gamma[\Delta, \Lambda]$ enables us to derive the inverse of the composite propagators matrix, defined for constant Δ and Λ , and its Fourier transform, $\Gamma(p)$ can be diagonalized. In Figs. ?? and ?? we show the Feynman diagram representations for the inverse of the two-particle propagator, $\Gamma^4(p)$ (up to \hbar^3), and for that of the four-particle propagator, $\Gamma^8(p)$ (up to \hbar^2), respectively.

For constant Δ and Λ , J_0 , K_0 and Ω are also space-time independent, thus (31) becomes (28), and (34) can be written as

$$\Lambda = \Lambda_{(0)}(J_0, K_0)$$

$$= (K_0 - 24\lambda) \int \frac{d^n p d^n q d^n r}{(2\pi)^{3n} (p^2 + \Omega^2)(q^2 + \Omega^2)(r^2 + \Omega^2)((p+q+r)^2 + \Omega^2)} \quad (37)$$

and inverted to obtain

$$K_0 = 24\lambda + \frac{\Lambda}{\int \frac{d^n p d^n q d^n r}{(2\pi)^{3n} (p^2 + \Omega^2)(q^2 + \Omega^2)(r^2 + \Omega^2)((p+q+r)^2 + \Omega^2)}}. \quad (38)$$

The relations (28) and (38) can be used to eliminate Δ and K_0 in favor of Ω and Λ in the calculated quantities. The values Ω and Λ have to be determined from the gap equations (5) and (6), which become algebraic.

3 The quantum-mechanical anharmonic oscillator

In the space-time of one dimension the $\lambda\Phi^4$ theory is equivalent to the quantum mechanical anharmonic oscillator with a Hamiltonian given by

$$H = \frac{1}{2}p^2 + \frac{1}{2}m^2x^2 + \lambda x^4. \quad (39)$$

The exact element of the composite propagator matrix in the Euclidean formulation can be represented as

$$\begin{aligned} W_{ij}(t-t') &= \ll 0 | T x^i(t) x^j(t') | 0 \gg - \ll 0 | x^i(t) | 0 \gg \ll 0 | x^j(t') | 0 \gg \\ &= \sum_{k=1}^{\infty} \ll 0 | x^i | k \gg \ll k | x^j | 0 \gg e^{-|t-t'|\epsilon_k}, \end{aligned} \quad (40)$$

where $\epsilon_k = E_k - E_0$ is the excitation energy of the k -th state, $|k \gg$. The Fourier transform of the above propagator is given by

$$W_{ij}(p) = \sum_{k=1}^{\infty} \frac{2\epsilon_k \ll 0 | x^i | k \gg \ll k | x^j | 0 \gg}{p^2 + \epsilon_k^2}, \quad (41)$$

and has an infinite number of poles at imaginary momenta whose absolute values determine all excitations of the system. Equivalently the full spectrum can be obtained by looking for zero modes of the exact inverse propagator matrix, $\Gamma(p)$. However, if we are working with an approximate propagator, which may have only a finite number of poles, this provides an approximation to some part of the energy spectrum only. Different, but usually better, approximations can be obtained from zero modes of the Γ matrix, and such an approach will be used in our work.

3.1 The approximations of the AO spectrum

3.1.1 The approximations derived from $\Gamma[\Delta]$

The vacuum energy density of the scalar field in the one dimensional space-time gives the ground state energy of the AO. Using the effective action for the operator Φ^2 , $\Gamma[\Delta]$, given in Fig. ?? the ground state energy of the AO is calculated to be

$$E_0 = \hbar \frac{\Omega}{2} - (\Omega^2 - m^2) \hbar \frac{\Delta}{2} + 3\lambda \hbar^2 \Delta^2 - \frac{3\lambda^2 \hbar^3}{8\Omega^5} + \frac{27\lambda^3 \hbar^4}{16\Omega^8} - \frac{1923\lambda^4 \hbar^5}{128\Omega^{11}} + \dots \quad (42)$$

where Δ is space-time independent, and by Eq. (28) is given by

$$\Delta = \frac{1}{2\Omega}. \quad (43)$$

The two-particle inverse propagator, from Fig. ??, becomes equal to

$$\begin{aligned} -\Gamma^4(p) = & \frac{\Omega}{2}(p^2 + 4\Omega^2) + 6\lambda\hbar - 3\lambda^2\hbar^2 \frac{160\Omega^2 + p^2}{\Omega^3(16\Omega^2 + p^2)} + 27\lambda^3\hbar^3 \frac{7168\Omega^4 + 176\Omega^2 p^2 + p^4}{2\Omega^6(16\Omega^2 + p^2)^2} \\ & - 3\lambda^4\hbar^4 \frac{5198561280\Omega^8 + 416746496\Omega^6 p^2 + 11879232\Omega^4 p^4 + 160692\Omega^2 p^6 + 641p^8}{16\Omega^9(16\Omega^2 + p^2)^3(36\Omega^2 + p^2)} + \dots \end{aligned} \quad (44)$$

and its zero determined to the order \hbar^4 results in an approximation to the second excitation given by

$$\epsilon_2 = 2\Omega + \frac{3\hbar\lambda}{\Omega^2} - \frac{87\hbar^2\lambda^2}{4\Omega^5} + \frac{2547\hbar^3\lambda^3}{8\Omega^8} - \frac{401691\hbar^4\lambda^4}{64\Omega^{11}} + \dots \quad (45)$$

The effective mass Ω has to be determined from the gap equation (5) which, after using (43), in the one-dimensional space-time becomes

$$32\Omega^{12} - 32m^2\Omega^{10} - 192\lambda\hbar\Omega^9 + 240\lambda^2\hbar^2\Omega^6 - 1728\lambda^3\hbar^3\Omega^3 + 21153\lambda^4\hbar^4 + \dots = 0. \quad (46)$$

It is important to notice here that the non-perturbative character of the approximations studied in this work is due to non-perturbative treatment of the gap equation - working with an effective action at a given order in \hbar the gap equation will be truncated to that order in \hbar and solved after setting $\hbar = 1$. One can easily check that if one expanded the solution of the gap equation Ω to the given order in \hbar , the results for the ground state

energy and for the second excitation would coincide to that order in λ with energies obtained in perturbation theory for Schrödinger equation. A field-theoretical derivation of the perturbative result for the second excitation in the loop expansion of the conventional effective action is considerably more laborious, since more diagrams have to be evaluated [1].

In this approach approximations to higher excitations cannot be obtained, because composite propagators for higher number of particles cannot be derived directly from $\Gamma[\Delta]$. There is however another strategy, analogous to Brillouin-Wigner perturbation theory, which seems to provide a way out, by calculating all zeros in the expression for $\Gamma^4(p)$ of this order, and treating them as approximations to successive excitations. We have checked that the lowest zero of $\Gamma^4(p)$ provides a good approximation to the second excitation, and in this case the result is close to (45). However, the other zeros do not agree with the exact results: the higher the excitation, the worse the agreement. Even the perturbative behavior of the excitations, obtained by using a solution of the gap equation expanded to the given order in \hbar , is wrong. In fact, the Brillouin-Wigner strategy applied to the two-particle inverse propagator is not able to provide reasonable approximations for higher excitations and does not show any supremacy over the Rayleigh-Schrödinger strategy. Therefore, in our work we use the Rayleigh-Schrödinger strategy, approximating excitation energies by zeros of the composite propagators calculated to the considered order in \hbar . In this approach higher excitations can be investigated by considering the effective actions for higher composite operators which directly generate higher composite propagators.

3.1.2 The approximations derived from $\Gamma[\Delta, \Lambda]$

We shall derive an approximation to the AO spectrum from the effective action for $\Phi^2(x)$ and $\Phi^4(x)$, $\Gamma[\Delta, \Lambda]$, discussed in Section (2.3). Calculating the Feynman diagrams of Fig. ?? in the space-time of one dimension the ground state energy is obtained in the form

$$E_0 = \hbar \frac{\Omega}{2} - (\Omega^2 - m^2) \hbar \frac{\Delta}{2} + 3\lambda \hbar^2 \Delta^2 + \frac{2}{3} \Lambda^2 \hbar^3 \Omega^5 + \hbar^3 \lambda \Lambda - 4\Lambda^3 \hbar^4 \Omega^7 + \dots, \quad (47)$$

where (43) can be used to eliminate Δ in favor of Ω . The inverse two-particle propagator, taken from Fig. ??, in one-dimensional space-time becomes

$$\begin{aligned}\Gamma^4(p) &= \frac{\Omega}{2}(p^2 + 4\Omega^2) + 6\lambda\hbar - 16\Lambda^2\Omega^7\hbar^2 \frac{160\Omega^2 + p^2}{3(16\Omega^2 + p^2)} \\ &+ 64\hbar^3\Lambda^3\Omega^9 \frac{256\Omega^4 + 176\Omega^2p^2 + p^4}{(16\Omega^2 + p^2)^2} + \dots,\end{aligned}\quad (48)$$

and its zero, calculated to order \hbar^3 , determines the second excitation to be

$$\epsilon_2 = 2\Omega + \frac{3\lambda\hbar}{\Omega^2} - 104\frac{\Lambda^2\hbar^2\Omega^5}{3} - \frac{9\lambda^2\hbar^2}{4\Omega^5} - 96\Lambda^3\hbar^3\Omega^7 + 20\Lambda^2\hbar^3\Omega^2\lambda + \frac{27\lambda^3\hbar^3}{8\Omega^8} + \dots(49)$$

The inverse four-particle propagator, from Fig. ??, takes the form

$$\begin{aligned}\Gamma^8(p) &= 2\Omega^3(16\Omega^2 + p^2) + \hbar(32\Omega^5 - 576\Lambda\Omega^7 + 2\Omega^3p^2 - 12\Lambda\Omega^5p^2) \\ &+ \frac{\hbar^2}{9(4\Omega^2 + p^2)(36\Omega^2 + p^2)} \left(41472\Omega^9 - 746496\Lambda\Omega^{11} - 331776\Lambda^2\Omega^{13} \right. \\ &+ 14112\Omega^7p^2 - 222912\Lambda\Omega^9p^2 + 544384\Lambda^2\Omega^{11}p^2 + 1008\Omega^5p^4 - 9504\Lambda\Omega^7p^4 \\ &+ 32768\Lambda^2\Omega^9p^4 + 18\Omega^3p^6 - 108\Lambda\Omega^5p^6 + 88\Lambda^2\Omega^7p^6 \left. \right) + \dots\end{aligned}\quad (50)$$

and its zero, calculated to order \hbar^2 , determines the fourth excitation to be

$$\epsilon_4 = 4\Omega - 24\Lambda\hbar\Omega^3 - \frac{560\Lambda^2\hbar^2\Omega^5}{3} + \dots\quad (51)$$

In the above expressions the effective mass, Ω , and the effective coupling, Λ , are space-time independent and have to be determined from the gap equations (5) and (6), which in one-dimensional space-time become

$$m^2 - \Omega^2 - 8\hbar\Lambda\Omega^4 + \frac{176\hbar^2\Lambda^2\Omega^6}{3} - \frac{400\hbar^3\Lambda^3\Omega^8}{9} + \dots = 0\quad (52)$$

$$24\hbar\lambda + 32\hbar\Lambda\Omega^5 - 288\hbar^2\Lambda^2\Omega^7 + \frac{5632\hbar^3\Lambda^3\Omega^9}{9} \dots = 0\quad (53)$$

When considering the approximations to the AO spectrum at a given order, we shall truncate these equations to that order in \hbar , and solve them after setting $\hbar = 1$. If one expanded instead the solutions of the gap equations, Ω and Λ , in powers of \hbar , the perturbative results for the ground state energy and the second excitation to order λ^3 and for the fourth excitation to order λ^2 would be recovered.

3.2 The numerical results for the AO energy levels

Here we shall compare the numerical results for the AO spectrum, obtained from $\Gamma[\Delta]$, with those from $\Gamma[\Delta, \Lambda]$. With the use of $\Gamma[\Delta]$ only the ground state and the second excitation can be calculated, but $\Gamma[\Delta, \Lambda]$ enables us to obtain in addition the fourth excitation. Both methods are non-perturbative, since the gap equations truncated to the given order in \hbar have been solved numerically, after setting $\hbar = 1$. In both cases the solution with the largest positive value for Ω has been chosen. The results are compared with the exact values of the AO energy levels, calculated by a numerical procedure based on a modification of the linear variational method [17], and with the results of perturbation theory. All results are presented as functions of the dimensionless quantity $z = \frac{m^2}{2\lambda^{2/3}}$, which is the only parameter of the theory after rescaling all quantities in terms of λ .

In Fig.10 we present the results for the ground state energy to successive orders in \hbar . The quality of an approximation can be expressed in terms of a critical value of the parameter z , below which large discrepancies between results of different orders and the exact value appear. The critical value for approximations (42) obtained from $\Gamma[\Delta]$, $z_{crit} \approx -1.$, appears much smaller than that for the perturbative results, $z_{crit} \approx 2.$. The approximations (47), obtained from $\Gamma[\Delta, \Lambda]$, are still better hence the critical value is still smaller, $z_{crit} \approx -3.$

The results for the second excitation, shown in Fig.11, are very similar to those for the ground state, only the critical values are correspondingly larger: $z_{crit} \approx 4.$ for the perturbative calculations, $z_{crit} \approx 2.$ for the approximations obtained from $\Gamma[\Delta]$ (45), and $z_{crit} \approx -0.5$ for that obtained from $\Gamma[\Delta, \Lambda]$ (??). These results should be compared with those obtained in the same order of the 2PPI expansion [10]. We observe that the two methods of expanding $\Gamma[\Delta]$ provide the approximations to the AO spectrum of a similar quality.

The approximations for the fourth excitation can be obtained from the inverse four-particle propagator $\Gamma^8(p)$, which can be derived directly from $\Gamma[\Delta, \Lambda]$, but not from $\Gamma[\Delta]$. As can be seen in Fig.12 the results (51), obtained from $\Gamma[\Delta, \Lambda]$, are in good agreement with the exact result for the values of the parameter z greater than $z_{crit} \approx 1.$ This should be compared with the perturbative results where $z_{crit} \approx 5.$

It is interesting to observe that $\Gamma[\Delta]$ and $\Gamma[\Delta, \Lambda]$ provide reasonable results for ground state energy even in the case of the double-well anharmonic

potential ($z < 0$), if the wells are not too deep. Since the results derived from $\Gamma[\Delta, \Lambda]$ are considerably better, one may suppose that including higher composite operator could improve the convergence properties and make the method applicable even in the case of deeper wells. In all methods considered the numerical results for the excitations are worse than that for the ground state: the higher the excitation, the larger the critical values below which the method does not converge, but in any case including the operator Φ^4 improves the convergence. One can speculate that increasing the number of composite operators included in the effective action, we could make the method applicable for higher excitations in the case of the double well potential.

4 Conclusions

In the quantum scalar field theory the effective action for the local composite operator $\Phi^2(x)$, $\Gamma[\Delta]$, can be obtained by performing the Legendre transform of the connected generating functional $W[J]$ order by order in \hbar . This provides a convenient tool to study the ground state and the second excitation in the theory. The result to the order \hbar^2 coincides with the Gaussian approximation, where the effective propagator is a Hartree one; higher orders provide a way to go beyond this result. A further improvement of the method can be achieved by taking into consideration higher composite operators $\Phi^k(x)$; their effects appear successively in higher orders of \hbar .

In this work we investigated the effects of including the operator $\Phi^4(x)$ in the effective action, $\Gamma[\Delta, \Lambda]$, which has been calculated as a series in \hbar . The effects of the operator $\Phi^4(x)$ first appear at order \hbar^3 . The successive approximations for the energy density and for the inverses of the two- and four-particle propagators, $\Gamma^4(p)$ and $\Gamma^8(p)$ have been derived from $\Gamma[\Delta, \Lambda]$. To each order in \hbar the effective mass and coupling have to be determined from the algebraic gap equations. The numerical results for the ground state and lowest excitations have been calculated for the theory in the space-time of one dimension, i.e., for quantum mechanical anharmonic oscillator. In this case the gap equations were solved numerically, and the excitation energies were determined as zeros of the inverse composite propagators in successive orders of \hbar . A comparison with the results obtained from the effective action for the operator $\Phi^2(x)$, $\Gamma[\Delta]$, shows that including the operator $\Phi^4(x)$ improves

the convergence of the approximation to the ground and the second excitation considerably. Moreover, the effective action $\Gamma[\Delta, \Lambda]$ enables us to obtain the approximation to the fourth excitation which is not possible with the use of $\Gamma[\Delta]$.

One may note that the Gaussian approximation, obtained as the lowest approximation to the effective action for the operator $\Phi^2(x)$, appears also in a variational calculation with the Gaussian trial propagator. However, it is not straightforward to obtain a substantial improvement beyond the result of this simple ansatz by modification of the trial propagator [18]. Including higher operators into the effective action provides such a improvement, and in addition enables one to study excitations of the system.

References

- [1] A.Okopińska, Annals of Physics (N.Y.) **228** (1993) 19.
- [2] T.D.Lee and C.N.Yang, Phys. Rev. **117** (1960) 22.
- [3] C.de Dominicis and P.C.Martin, J. Math. Phys. **5** (1964) 14,31.
- [4] A.N.Vasil'ev and A.K.Kazanskii, Teor.Mat.Fiz.**19** (1974) 186.
- [5] J.M.Cornwall, R.Jackiw, and E.Tomboulis, Phys. Rev. **D10** (1974) 2428.
- [6] T.Barnes and G.I.Ghandour, Phys.Rev.**D22** (1980) 924; P.M.Stevenson, Phys. Rev. **D32** (1985) 1389.
- [7] R.Fukuda, Prog. Theor. Phys. **78** (1987) 1487.
- [8] H.J.He and Y.P.Kuang, Zeit. Phys. **C47** (1990) 565.
- [9] H.Vershelde and M.Coppens, Phys. Lett. **B287** (1992) 133.
- [10] A.Okopińska, Annals of Physics (N.Y.) to appear.
- [11] K.Okumura, Int.J.Mod.Phys.**A11**(1995) 65;
- [12] H.Vershelde, private communication.
- [13] R.Fukuda, Phys. Rev. Lett. **61** (1988) 1549; M.Ukita, M.Komachiya, and R.Fukuda, Int.J.Mod.Phys.**A5** (1990) 1789; R.Fukuda, Phys.Rev.**B46** (1992) 10931.
- [14] S.Yokojima, Phys.Rev.**D51** (1995) 2996.
- [15] R.Fukuda, M.Komachiya, and M.Ukita, Phys.Rev.**D38** (1988) 3747.
- [16] R.Fukuda, Prog. Theor. Phys. **92** (1994) 863;
- [17] A.Okopińska, Phys. Rev. **D36** (1987) 1273.
- [18] B.Bellet, P.Garcia, and A.Neveu, hep-th/9507155.

Figure captions

Figure 1. The loop expansion of $W[J, K]$ in terms of Feynman diagrams in configuration space; the line denotes the propagator $(-\partial^2 + \Omega^2(x))^{-1}\delta(x - y)$, and the full circle stands for the four-particle coupling $(-24\lambda + K(x))\delta(x - y)\delta(x - w)\delta(x - z)$.

Figure 2. $\Delta[J, K]$ and $\Lambda[J, K]$ represented with Feynman rules of Fig.1; the small empty circle denotes an external point x .

Figure 3. $J[\Delta]$ obtained by inversion of $\Delta[J]$ in powers of \hbar . The line denotes the propagator $(-\partial^2 + \Omega^2(x))^{-1}\delta(x - y)$ and the four-particle vertex is $-24\lambda\delta(x - y)\delta(x - w)\delta(x - z)$. Two lines meeting at two points with the slash across represent the inverse of the free two-particle propagator.

Figure 4. $\Gamma[\Delta]$ represented with Feynman rules of Fig.3.

Figure 5. The inverse of the two-particle propagator, calculated from $\Gamma[\Delta]$, represented in terms of Feynman diagrams in momentum space; the line stands for a free propagator $\frac{1}{p^2 + \Omega^2}$, the small empty circle denotes an external momentum p .

Figure 6. $J[\Delta, \Lambda]$ and $K[\Delta, \Lambda]$ obtained by inversion of $\Delta[J, K]$ and $\Lambda[J, K]$ in powers of \hbar ; the single line denotes the propagator $(-\partial^2 + m^2 - J_0(x))^{-1}\delta(x - y)$, the lines meeting at two points represent the free composite propagator of the corresponding number of fields, and the slash means the inversion.

Figure 7. $\Gamma[\Delta, \Lambda]$ represented with Feynman rules of Fig.6.

Figure 8. The inverse of the two-particle propagator, calculated from $\Gamma[\Delta, \Lambda]$, represented in terms of Feynman diagrams in momentum space; the line stands for a free propagator $\frac{1}{p^2 + \Omega^2}$, the small circle denotes an external momentum p .

Figure 9. As Fig.8, but for the inverse of the four-particle propagator, calculated from $\Gamma[\Delta, \Lambda]$.

Figure 10. The ground state energy of the AO, obtained to the given order of \hbar from $\Gamma[\Delta]$ (*dotted lines*) and from $\Gamma[\Delta, \Lambda]$ (*dotted-dashed lines*), plotted *vs* $z = \frac{m^2}{2\lambda^{2/3}}$; compared with the exact value (*solid lines*) and given order perturbative results (*dashed lines*).

Figure 11. As in Fig.10, but for the second excitation energy of the AO.

Figure 12. As in Fig.10, but for the fourth excitation energy of the AO.

$$\begin{aligned}
W[J, K] = & -\frac{\hbar}{2} \text{ (single circle) } + \frac{\hbar^2}{8} \text{ (two circles connected at a point) } + \frac{\hbar^3}{48} \text{ (circle with two internal lines) } + \frac{\hbar^3}{16} \text{ (three circles connected at a point) } \\
& + \frac{\hbar^4}{48} \text{ (circle with three internal lines forming a triangle) } + \frac{\hbar^4}{32} \text{ (three circles connected in a chain) } + \frac{\hbar^4}{48} \text{ (circle with four internal lines forming a star) } + \frac{\hbar^4}{24} \text{ (circle with two internal lines and a bubble) } + \frac{\hbar^5}{32} \text{ (circle with four internal lines forming a square) } \\
& + \frac{\hbar^5}{128} \text{ (circle with four internal lines forming a square with diagonals) } + \frac{\hbar^5}{64} \text{ (four circles connected in a chain) } + \frac{\hbar^5}{128} \text{ (circle with five internal lines forming a star) } + \frac{\hbar^5}{32} \text{ (three circles connected in a chain with a bubble) } \\
& + \frac{\hbar^5}{144} \text{ (circle with four internal lines forming a square with diagonals and a bubble) } + \frac{\hbar^5}{16} \text{ (circle with three internal lines forming a triangle and a bubble) } + \frac{\hbar^5}{48} \text{ (circle with two internal lines and two bubbles) } + \frac{\hbar^5}{32} \text{ (circle with two internal lines and a bubble) } + \frac{\hbar^5}{48} \text{ (circle with two internal lines and a bubble) } + \dots
\end{aligned}$$

Figure 1: The loop expansion of $W[J, K]$ in terms of Feynman diagrams in configuration space; the line denotes the propagator $(-\partial^2 + m^2 - J(x))^{-1} \delta(x - y)$, and the full circle stands for the four-particle coupling $(-24\lambda + K(x)) \delta(x - y) \delta(x - w) \delta(x - z)$.

$$\begin{aligned}
\Delta[J, K] = & \text{[Diagram: circle with external point]} + \frac{\hbar}{2} \text{[Diagram: two circles with external point]} + \frac{\hbar^2}{6} \text{[Diagram: circle with internal loop and external point]} + \frac{\hbar^2}{4} \text{[Diagram: three circles with external point]} \\
& + \frac{\hbar^2}{4} \text{[Diagram: three circles with external point]} + \frac{\hbar^3}{8} \text{[Diagram: three circles with external point]} + \frac{\hbar^3}{4} \text{[Diagram: three circles with external point]} + \frac{\hbar^3}{8} \text{[Diagram: three circles with external point]} \\
& + \frac{\hbar^3}{8} \text{[Diagram: three circles with external point]} + \frac{\hbar^3}{4} \text{[Diagram: triangle with external point]} + \frac{\hbar^3}{12} \text{[Diagram: circle with internal loop and external point]} + \frac{\hbar^3}{6} \text{[Diagram: circle with internal loop and external point]} + \frac{\hbar^3}{4} \text{[Diagram: circle with internal loop and external point]} + \dots \\
\Lambda[J, K] = & \text{[Diagram: circle with internal loop and external point]} + \frac{3\hbar}{2} \text{[Diagram: triangle with external point]} + 2\hbar \text{[Diagram: circle with internal loop and external point]} + \frac{3\hbar^2}{4} \text{[Diagram: square with external point]} + \frac{2\hbar^2}{3} \text{[Diagram: two vertical lines with external point]} \\
& + 3\hbar^2 \text{[Diagram: circle with internal loop and external point]} + 3\hbar^2 \text{[Diagram: triangle with external point]} + \frac{3\hbar^2}{2} \text{[Diagram: triangle with external point]} + \hbar^2 \text{[Diagram: circle with internal loop and external point]} + \frac{3\hbar^2}{2} \text{[Diagram: circle with internal loop and external point]} + \hbar^2 \text{[Diagram: circle with internal loop and external point]} + \dots
\end{aligned}$$

Figure 2: $\Delta[J, K]$ and $\Lambda[J, K]$ represented with Feynman rules of Fig.1; the small empty circle denotes an external point x .

$$\begin{aligned}
J[\Delta] = m^2 - \Omega^2[\Delta] + 12\hbar\lambda\Delta & - \text{diagram} \left[\frac{\hbar^2}{6} \text{diagram} + \frac{\hbar^3}{4} \text{diagram} \right. \\
& + \frac{\hbar^4}{8} \text{diagram} + \frac{\hbar^4}{36} \text{diagram} + \frac{\hbar^4}{12} \text{diagram} + \frac{\hbar^4}{4} \text{diagram} + \frac{\hbar^4}{4} \text{diagram} \\
& \left. - \frac{\hbar^4}{18} \text{diagram} - \frac{\hbar^4}{12} \text{diagram} + \frac{\hbar^4}{36} \text{diagram} + \dots \right]
\end{aligned}$$

where $\Delta = \text{diagram}$

Figure 3: $J[\Delta]$ obtained by inversion of $\Delta[J]$ in powers of \hbar . The line denotes the propagator $(-\partial^2 + \Omega^2(x))^{-1}\delta(x-y)$ and the four-particle vertex is $-24\lambda\delta(x-y)\delta(x-w)\delta(x-z)$. Two lines meeting at two points with a slash across represent the inverse of the free two-particle propagator.

$$\begin{aligned}
\Gamma[\Delta] = & \int [\frac{\hbar}{2}(\Omega^2(x) - m^2)\Delta(x) - 3\lambda\hbar^2\Delta^2(x)]dx - \frac{\hbar}{2} \text{ (circle) } + \frac{\hbar^3}{48} \text{ (circle with horizontal bar) } \\
& + \frac{\hbar^4}{48} \text{ (circle with triangle) } + \frac{\hbar^5}{128} \text{ (circle with square) } + \frac{\hbar^5}{32} \text{ (circle with two horizontal bars) } \\
& + \frac{\hbar^5}{144} \text{ (circle with two vertical bars) } - \frac{\hbar^5}{144} \text{ (circle with two vertical bars connected by a horizontal bar with a slash) }
\end{aligned}$$

Figure 4: $\Gamma[\Delta]$ represented with Feynman rules of Fig.3.

$$\begin{aligned}
-\Gamma^4(p) = & \frac{1}{2} \text{diagram} + 6\hbar\lambda - \text{diagram} \left[\begin{aligned}
& \frac{\hbar^2}{4} \text{diagram} + \frac{\hbar^2}{6} \text{diagram} - \frac{\hbar^2}{6} \text{diagram} + \frac{\hbar^3}{8} \text{diagram} + \frac{\hbar^3}{2} \text{diagram} \\
& + \frac{\hbar^3}{4} \text{diagram} - \frac{\hbar^4}{4} \text{diagram} + \hbar^4 \text{diagram} + \frac{\hbar^4}{16} \text{diagram} + \frac{\hbar^4}{4} \text{diagram} + \frac{\hbar^4}{4} \text{diagram} + \frac{\hbar^4}{6} \text{diagram} \\
& + \frac{\hbar^4}{8} \text{diagram} + \frac{\hbar^4}{8} \text{diagram} + \frac{\hbar^4}{4} \text{diagram} + \frac{\hbar^4}{8} \text{diagram} + \frac{\hbar^4}{4} \text{diagram} - \frac{\hbar^4}{18} \text{diagram} \\
& + \frac{\hbar^4}{12} \text{diagram} + \frac{\hbar^4}{4} \text{diagram} + \frac{\hbar^4}{4} \text{diagram} + \frac{\hbar^4}{8} \text{diagram} + \frac{\hbar^4}{12} \text{diagram} + \frac{\hbar^4}{72} \text{diagram} - \frac{\hbar^4}{4} \text{diagram} \\
& + \frac{\hbar^4}{36} \text{diagram} - \frac{\hbar^4}{8} \text{diagram} - \frac{\hbar^4}{4} \text{diagram} - \frac{\hbar^4}{12} \text{diagram} - \frac{\hbar^4}{36} \text{diagram} + \frac{\hbar^4}{9} \text{diagram} \\
& - \frac{\hbar^4}{12} \text{diagram} - \frac{\hbar^4}{6} \text{diagram} - \frac{\hbar^4}{12} \text{diagram} + \frac{\hbar^4}{6} \text{diagram} - \frac{\hbar^4}{36} \text{diagram} \\
& - \frac{\hbar^4}{6} \text{diagram} - \frac{\hbar^4}{8} \text{diagram} - \frac{\hbar^4}{18} \text{diagram} + \frac{\hbar^4}{12} \text{diagram} \\
& - \frac{\hbar^4}{18} \text{diagram} - \frac{\hbar^4}{36} \text{diagram} + \frac{\hbar^4}{18} \text{diagram} + \frac{\hbar^4}{72} \text{diagram} + \frac{\hbar^4}{36} \text{diagram} + \dots \end{aligned} \right] \text{diagram}
\end{aligned}$$

Figure 5: The inverse of the two-particle propagator, calculated from $\Gamma[\Delta]$, represented in terms of Feynman diagrams in momentum space; the line stands for a free propagator $\frac{1}{p^2+\Omega^2}$, the small empty circle denotes an external momentum p .

$$J[\Delta, \Lambda] = m^2 - \Omega^2(x) + 12\hbar\lambda\Delta(x) - \frac{\hbar}{2}\Delta K[\Delta, \Lambda]$$

$$- \text{[diagram: circle with two internal lines meeting at a point]} \left[\frac{\hbar^2}{6} \text{[diagram: circle with two internal lines meeting at two points]} + \frac{\hbar^3}{4} \text{[diagram: circle with three internal lines meeting at three points]} - \frac{\hbar^3}{2} \text{[diagram: circle with four internal lines meeting at four points]} + \dots \right]$$

$$K[\Delta, \Lambda] = 24\lambda + \text{[diagram: circle with two internal lines meeting at a point]} + \text{[diagram: circle with two internal lines meeting at two points]} \left[\frac{3\hbar}{2} \text{[diagram: circle with three internal lines meeting at three points]} + 3\hbar^2 \text{[diagram: circle with four internal lines meeting at four points]} + \frac{2\hbar^2}{3} \text{[diagram: circle with five internal lines meeting at five points]} \right. \\ \left. + \frac{3\hbar^2}{4} \text{[diagram: circle with six internal lines meeting at six points]} - \frac{2\hbar^2}{3} \text{[diagram: circle with seven internal lines meeting at seven points]} - \frac{9\hbar^2}{2} \text{[diagram: circle with eight internal lines meeting at eight points]} \right]$$

$$\text{where } \Delta = \text{[diagram: circle with one external line]} \text{ and } \text{[diagram: circle with two internal lines meeting at a point]} = \text{[diagram: circle with two internal lines meeting at two points]} \Lambda$$

Figure 6: $J[\Delta, \Lambda]$ and $K[\Delta, \Lambda]$ obtained by inversion of $\Delta[J, K]$ and $\Lambda[J, K]$ in powers of \hbar ; the single line denotes the propagator $(-\partial^2 + \Omega^2(x))^{-1}\delta(x-y)$, the lines meeting at two points represent the free composite propagator of the corresponding number of fields, and the slash means the inversion.

$$\Gamma[\Delta, \Lambda] = \int [\frac{\hbar}{2}(\Omega^2(x) - m^2)\Delta(x) - 3\lambda\hbar^2\Delta^2(x) - \hbar^3\lambda\Lambda(x)]dx$$

$$-\frac{\hbar}{2} \bigcirc - \frac{\hbar^3}{48} \bigcirc + \frac{\hbar^4}{48} \bigcirc + \dots$$

Figure 7: $\Gamma[\Delta, \Lambda]$ represented with Feynman rules of Fig.6.

$$\begin{aligned}
-\Gamma^4(p) = & \frac{1}{2} \text{ (diagram: circle with two external lines) } + 6\hbar\lambda \text{ (diagram: circle with two external lines and a cross) } \\
& \left[\frac{\hbar^2}{4} \text{ (diagram: circle with two internal lines) } + \frac{\hbar^2}{6} \text{ (diagram: circle with two internal lines and a cross) } - \frac{\hbar^2}{6} \text{ (diagram: circle with two internal lines and a cross) } \right. \\
& + \frac{\hbar^3}{4} \text{ (diagram: circle with two internal lines and a cross) } + \frac{\hbar^2}{2} \text{ (diagram: circle with two internal lines and a cross) } + \frac{\hbar^3}{8} \text{ (diagram: circle with two internal lines and a cross) } \\
& - \frac{\hbar^3}{2} \text{ (diagram: circle with two internal lines and a cross) } - \frac{\hbar^2}{4} \text{ (diagram: circle with two internal lines and a cross) } + \frac{\hbar^3}{2} \text{ (diagram: circle with two internal lines and a cross) } \\
& \left. - \frac{3\hbar^3}{4} \text{ (diagram: circle with two internal lines and a cross) } + \dots \right] \text{ (diagram: circle with two external lines) }
\end{aligned}$$

where $\times = \text{ (diagram: circle with two internal lines and a cross) } \Lambda$

Figure 8: The inverse of the two-particle propagator, calculated from $\Gamma[\Delta, \Lambda]$, represented in terms of Feynman diagrams in momentum space; the line stands for a free propagator $\frac{1}{p^2 + \Omega^2}$, the small circle denotes an external momentum p .

$$\begin{aligned}
-\Gamma^8(p) = & \frac{1}{24} \text{diagram} - \frac{1}{24} \text{diagram} \left[3\hbar \text{diagram} + \frac{3\hbar^2}{2} \text{diagram} + \frac{3\hbar^4}{4} \text{diagram} \right. \\
& + 3\hbar^2 \text{diagram} + \frac{2\hbar^2}{3} \text{diagram} + 6\hbar^2 \text{diagram} + \frac{2\hbar^2}{3} \text{diagram} - \frac{4\hbar^2}{3} \text{diagram} \\
& \left. - \frac{9\hbar^2}{2} \text{diagram} - 9\hbar^2 \text{diagram} + \frac{2\hbar^2}{3} \text{diagram} - \frac{2\hbar^2}{3} \text{diagram} + \dots \right] \text{diagram}
\end{aligned}$$

Figure 9: As Fig.8, but for the inverse of the four-particle propagator, calculated from $\Gamma[\Delta, \Lambda]$.

Figure 10

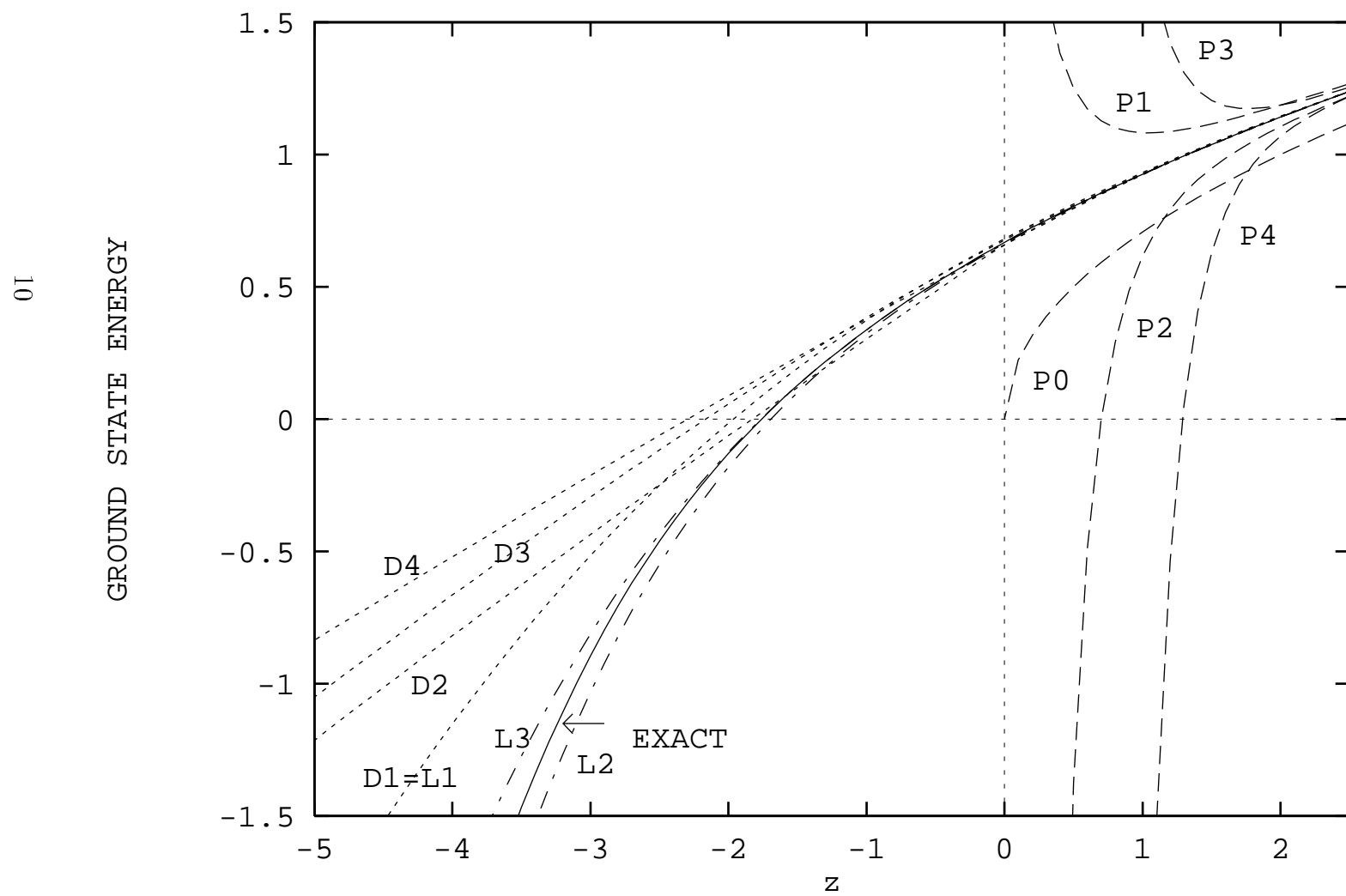


Figure 11

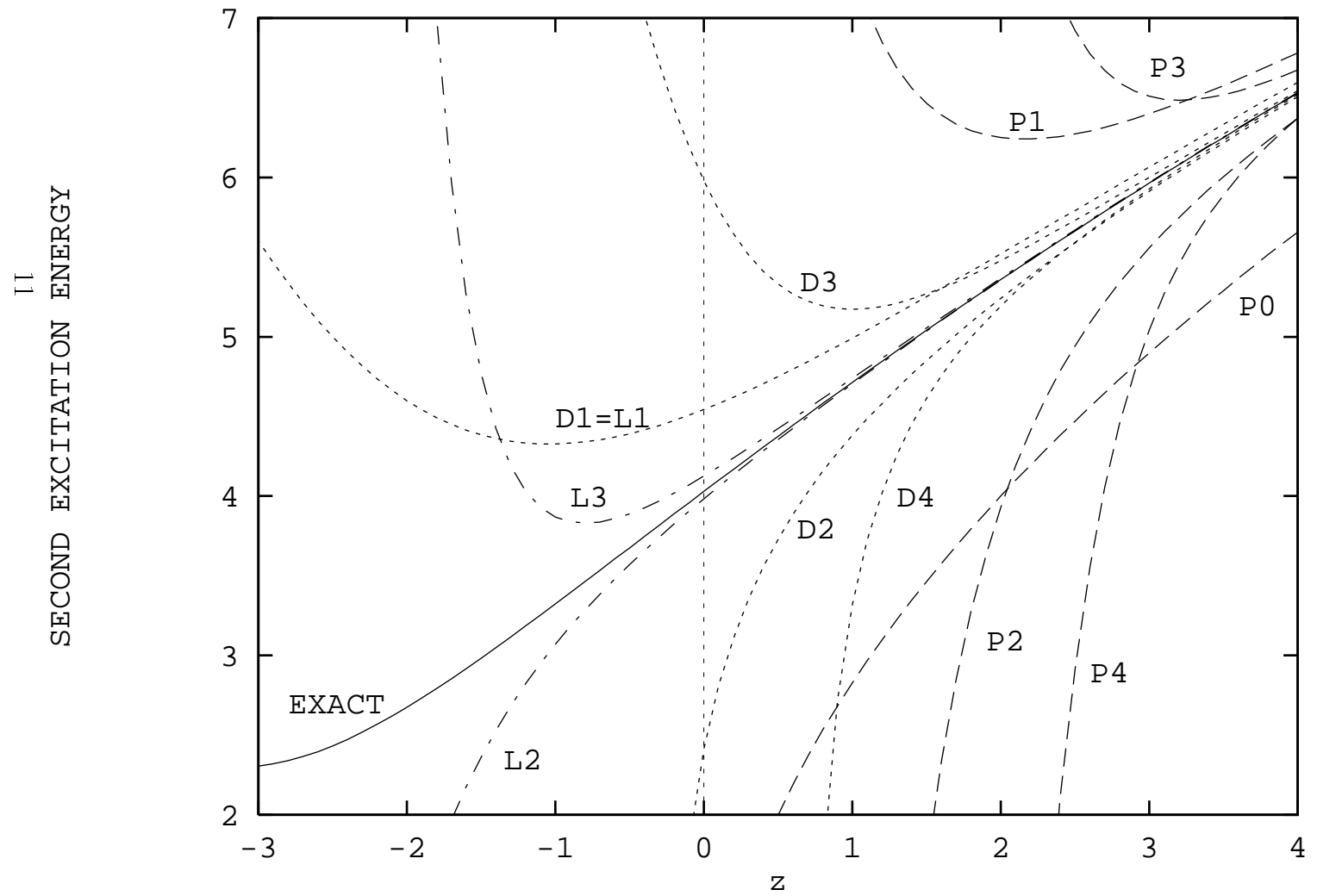


Figure 12

